

Fully Coupled Numerical Modelling of Wave-Current-Mud Interaction by Finite Volume Method

K. Hejazi, S. Sami & M. Soltanpour

Civil Eng. Dept., K.N.Toosi University of Tech., Tehran, Iran.

ABSTRACT: Wave-current-mud interaction is a complicated mechanism in the coastal and estuarine turbid waters. A laterally averaged finite volume numerical model has been used to study the interaction of wave, current and mud. The fully non-linear Navier-Stokes equations with complete set of kinematic and dynamic boundary conditions at free surface and interface and the Bingham constitutive equation for modelling the behavior of mud layer, are solved. Finite volume method based on an ALE description has been utilized for the simulation of wave motion in a combined system of water and mud layer. The model is applied for simulating three numerical tests including velocity profiles of steady flow along a trench, and variation of wave characteristics in interaction with opposing and following currents on fixed bed and mud bed. Comparison of the model predictions against analytical and experimental results confirms the ability of the model for wave-current-mud interaction predictions.

Keywords: Wave-Current-Mud Interaction, FVM, Bingham Equation, ALE, Projection Method

1 INTRODUCTION

Historically, sediments have been treated as either muds or sands due to the different characteristics and consequent behaviour for each of them. Muddy sediments occur commonly in estuaries, coastal embayment, and in areas of the continental shelf where both currents and waves exert only weak forces on the bed. Fluid mud is a highly concentrated near-bed suspension of cohesive sediments, with either mobile or stationary states. It is generated by liquefaction of muddy beds by waves, or during rapid deposition, when the deposition rate exceeds the consolidation rate.

Wave attenuation and mud mass transport are two noteworthy phenomena of wave-mud interaction, which have been observed both at laboratory and in field when waves propagate over muddy bottom, especially over low density mud beds. In addition to wave-mud interaction, introduction of currents in the wave field also affects wave propagation. The presence of currents would further complicate the phenomena of wave attenuation and mud mass transport by the interaction between waves and currents. Previous studies on wave-current-mud interaction are very limited. An (1993) presented a mathematical model based on a visco-elastic-plastic model of mud and conducted a series of wave flume experiments to clarify the interaction between wave-current and mud bed. The assumption of the no effect of mud bed on wave-current interaction and the assumption of the no direct effect of current on mud mass transport velocity, significantly simplify the mathematical formulation of wave-current-mud interaction problem. Based on these assumptions, the mathematical formulation of the wave-current-mud interaction problem in here study was divided into two steps. The first step was to determine the parameters of deformed wave such as the amplitude, wave number and relative angular frequency due to the current (after Thomas, 1981) in which the mud bed plays no role. The second step was to calculate the wave attenuation and mud mass transport in which actions of deformed waves were the only driving forces. By assuming separable and periodic solution, the two dimensionally linearized Navier-Stokes equations for multi-layered fluid were solved according to Tsuruya et al. (1987). The results revealed that the wave height variation due to wave-current interactions on the mud bed can be predicted by a simple model of irrotational slowly-varying current. It was reported that the wave attenuation increases in the opposing currents and decreases

in the following currents. The effect of currents on mud transport can be explained by the wave deformation due to current. In the opposing currents, the water pressure gradient at the water-mud interface becomes great as the wave height increases and the wavelength decreases, and this change causes to yield large mud transport. In the following currents, the pressure gradient becomes small as the wave height decreases and the wavelength increases and this results in small mud transport. In a numerical model presented by Zhao et al. (2006), the instantaneous velocity components and the instantaneous pressure of the Navier-stokes equations, were decomposed into the time-averaged components, periodic wave components and random pulsating components. By taking the time-average and the phase-average, in the case of combination of wave and current, and a number of scaling assumptions such as small wave amplitude and long wavelength, the current equation and the wave equation were obtained, respectively. Eddy viscosity models for wave and current were separately proposed to close the equation of wave or current motion in a combined flow on a visco-elastic mud layer, to model the wave height attenuation rate, distribution of current velocities in the water layer, distribution of transport velocities at the water-mud interface, and mud mass transport rate within the mud layer.

In this study the interaction of wave-current with a muddy bed bounded below by a horizontal rigid plane has been investigated by a laterally averaged numerical model. The numerical model is based on the fully nonlinear Navier-Stokes equations and the complete set of nonlinear free surface and interface boundary conditions. The capability of the model in accurately simulating the propagation of regular waves over fluid mud layer had been confirmed (Hejazi et al., 2013). The non-Newtonian behaviour of the mud layer is simulated by adding the constitutive equation of Bingham plastic to the governing equations. The numerical wave-mud interaction model is examined herein by the interactive wave-current and mud layer. The water wave attenuation has been computed under waves and is compared to the corresponding values reported in the experimental studies.

Application of the model in a system of combined wave and current over the mud-fluid bed shows good agreements in determining velocity profiles of current, free surface wave heights and wave lengths compared to the experimental data. The simulated wave height attenuation, as one major aspect of wave-mud interaction, shows good agreements compared to the measured data.

2 MATHEMATICAL FORMULATION

2.1 Governing Equations

Figure 1 shows the physical domain bounded by the moving free surface, $\eta_w(x,t)$, and the bottom boundary, $z = z_b(x)$. The upper layer is plain water subject to a wave disturbance and the lower layer is fluid mud.

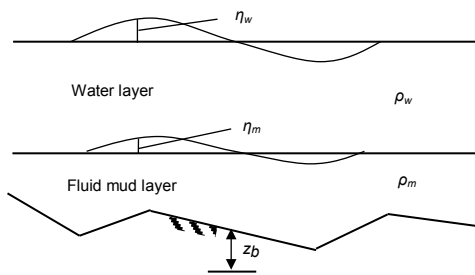


Figure 1. Schematic diagram of the two-layer viscous fluid system in the 2DV presentation.

The motion of an incompressible fluid in the two-dimensional vertical plane, at constant temperature is governed by the conservation equations of mass and momentum. The conservative form of equations in ALE (Arbitrary Lagrangian-Eulerian) description may be expressed as:

$$\frac{\partial u_i}{\partial x_i} = 0 \quad (1)$$

$$\frac{\partial u_i}{\partial t} + \frac{\partial u_i u_j}{\partial x_j} - u_g \frac{\partial u_i}{\partial x_j} = -\frac{\rho_r}{\rho} \frac{\partial P^*}{\partial x_i} + \frac{1}{\rho} \frac{\partial \tau_{ij}}{\partial x_j} - \left(\frac{\rho - \rho_r}{\rho} \right) g \quad (2)$$

where t = time, x = the Cartesian coordinate, u = the velocity, P^* = the pressure in the absence of hydrostatic pressure divided by reference density of water, ρ = the fluid density, ρ_r = the reference density of water, τ = the symmetric extra-stress tensor, g = the gravitational acceleration, and u_g = the vertical mesh

velocity obtained from the vertical displacement of mesh in each time step which only appears for $j = 2$. The indices $i, j = 1, 2$ represent the coordinate directions. The last term of equation (2) is only included for $i = 2$.

To complete the formulation, a constitutive equation to represent the physical properties of the continuum, must be added. For Newtonian fluids, the viscosity, μ , is assumed to be independent of shear rate tensor. The relation between the stress tensor and the shear rate tensor, $\dot{\gamma}_{ij}$, is expressed as:

$$\tau_{ij} = \mu \dot{\gamma}_{ij} \quad (3)$$

$$\dot{\gamma}_{ij} = \frac{\partial u_i}{\partial x_j} + \frac{\partial u_j}{\partial x_i} \quad (4)$$

Different constitutive equations have been assumed for prediction of the response of muddy beds due to complexity of the mud behavior. To model the stress-deformation of Bingham plastic behaviour of fluid mud, the ideal Bingham constitutive equations have been proposed as:

$$\begin{aligned} \tau_{ij} &= \tau_y + \mu_B \dot{\gamma}_{ij}, & \text{for } |\tau_{ij}| > \tau_y \\ \dot{\gamma}_{ij} &= 0, & \text{for } |\tau_{ij}| \leq \tau_y \end{aligned} \quad (5)$$

where τ_y = the yield stress, and μ_B = the plastic viscosity. These constitutive relations indicate that when the magnitude of the local stress falls below τ_y , the material is unyielded and behaves like a solid, and once it is yielded, fluid motion is launched. To avoid the discontinuity inherent in this model, Papanastasiou (1987) proposed a modified expression that makes the shear stress vary continuously with the shear rate as:

$$\tau_{ij} = \tau_y [1 - \exp(-m \dot{\gamma}_{ij})] + \mu_B \dot{\gamma}_{ij} \quad (6)$$

where m = the material parameter which controls the exponential growth of the stress. The ideal Bingham fluid can be closely approximated if m is large enough. Equation (6) can be rewritten as:

$$\tau_{ij} = \left(\mu_B + \frac{\tau_y}{|\dot{\gamma}_{ij}|} [1 - \exp(-m |\dot{\gamma}_{ij}|)] \right) \dot{\gamma}_{ij} \quad (7)$$

where $|\dot{\gamma}_{ij}|$ = the second invariant of the rate-of-strain tensor whose magnitude can be calculated through

$$|\dot{\gamma}_{ij}| = \sqrt{\frac{1}{2} \text{tr } \dot{\gamma}_{ij}^2} \quad (8)$$

The resulting momentum equations for the Bingham plastic fluid mud can be obtained by substituting Equation (7) in (2) that yields:

$$\frac{\partial u_i}{\partial t} + \frac{\partial u_i u_j}{\partial x_j} - u_g \frac{\partial u_i}{\partial x_j} = -\frac{\rho_r}{\rho} \frac{\partial P^*}{\partial x_i} + \frac{1}{\rho} \frac{\partial}{\partial x_j} \left\{ \mu_B + \frac{\tau_y}{|\dot{\gamma}_{ij}|} [1 - \exp(-m |\dot{\gamma}_{ij}|)] \right\} \dot{\gamma}_{ij} - \left(\frac{\rho - \rho_r}{\rho} \right) \delta_{i2} g \quad (9)$$

2.2 Boundary Conditions

Spatial boundary conditions have been divided into five locations: the rigid bottom of the mud layer (bed), the interface boundary at plain water and mud flow, the free surface of water, the inlet, and the outlet boundaries (Hejazi et al., 2013).

3 NUMERICAL METHOD

The numerical model uses a structured non-orthogonal curvilinear staggered mesh and is capable of simulating non-homogeneous, gravity stratified flow fields. Projection method has been deployed for solving the non-hydrostatic Reynolds-averaged Navier–Stokes equations based on an ALE description. With finite volume method in the ALE system, the newly updated free surface is determined purely by the Lagrangian method, and by the velocity of the fluid particles at the free surface, while the nodes in the interior of the domain are displaced in an arbitrary prescribed manner to be redistributed to avoid mesh crossing. To solve the set of the equations, in the first step the pressure gradient terms are omitted from the momentum equations, and the unsteady equations which include the advective and diffusive terms, are advanced in time to obtain a provisional velocity field. For large Reynolds numbers, the flow is effectively advection-dominated; hence, to achieve more realistic predictions of the flow characteristics, the

advection part of the transport has been examined by assuming a fourth-degree polynomial as the shape function of the quantity to be advected, providing a fifth-order accurate scheme (Hejazi 2005). In the second step the provisional velocity is corrected by accounting for the pressure gradient and the continuity constraint. The water elevation is computed through the solution of the free surface equation obtained from the application of normal and tangential dynamic boundary conditions, and the integration of the continuity equation over the water depth. The interface elevation is obtained by the application of the integration of the continuity equation over the mud layer depth, and the kinematic boundary conditions at bed and interface. The mesh is re-generated at each time step in mud and water layers independently. In the mud layer, grid geometry is computed and updated according to the interface and bed levels, whereas in the water layer, the grid is updated according to the interface and free surface levels. The apparent viscosity of fluid mud, the expression in bracket in Equation (9), has been calculated explicitly, based on the values of velocity field at the previous time step.

4 MODEL VALIDATIONS

To validate the model for wave-current interaction, two hydrodynamic tests including a current flow over a trench and the wave current interaction on a fixed bed have been carried out. Predicted values of the current flow over the trench have been compared with the corresponding experimental measurements for velocity distribution. The simulated values of variation of wave height and wave length caused by interaction with a following and opposing current in a constant water depth have been compared against the theoretical solution. For wave-current-mud interaction a two-layer system in which a layer of clear water overlies a thin layer of mud was considered. The predicted values of height and length of wave have been compared versus measured values. The wave damping coefficients have also been compared with the experimental based values. The mass transport velocity has been computed and compared with experimental based data.

4.1 Current Flow over a Trench

A steady current flow over a trench is simulated and the numerical results are compared with experimental data of Alfrink and van Rijn (1983). The measurements have been carried out in a 17 m long and 0.7 m deep flume which comprises a trench of 0.2 m depth with a base length of 1 m and side slopes of 1:2. A discharge per unit width of $0.08 \text{ m}^2/\text{s}$ was pumped in from the left-hand side and the same discharge was pumped out from the right end of the flume. A length of 7.5 m is considered for the simulation domain with a known discharge at the left- and right-hand boundaries. Space and time intervals and the number of computational layers are set to 0.04 m, 0.01 s and 20 respectively. The steady current flow is simulated for the water depth of 0.2 m. To avoid the creation of any wave reflections, the inlet discharge is increased linearly from zero to $0.08 \text{ m}^2/\text{s}$ after 250 s of simulation time, at which it remains constant. The steady state solution is obtained after 500 s. The two-equation buoyant k- ϵ model is employed to calculate the distribution of the eddy viscosity in the domain. Figure 2 presents the comparison of the predicted horizontal velocity components against the measurements at five cross-sections, positioned at stations A (-1.1 m), B (-0.7 m), C (0.0), D (0.7 m), and E (1.3 m) from the middle of the trench. The numerical results agree well with experimental data.

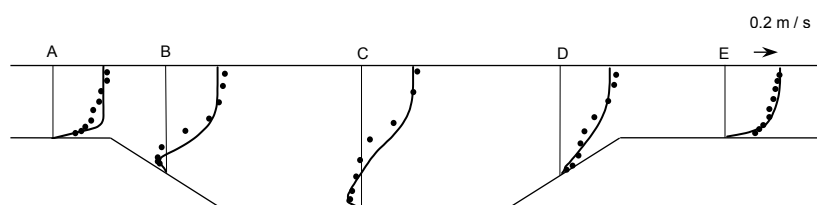


Figure 2. Steady flow over trench: comparison of predicted horizontal velocity components (solid lines) against experimental data (circles).

4.2 Wave-Current Interaction on a Fixed Bed

Propagation of wave and current in a constant water depth has been simulated to evaluate the wave deformation. No energy loss is considered. Two main parameters of deformed waves are the wave height and the wave length. Bretherton and Garrett (1969) derived a conservation equation for wave action, that is valid for waves traveling on a slowly varying current (i.e. the change of the current is small over a wave length):

$$\frac{\partial}{\partial t} \left(\frac{E}{\omega} \right) + \nabla \cdot \left\{ (\mathbf{U} + \mathbf{C}_g) \frac{E}{\omega} \right\} = 0 \quad (10)$$

where \mathbf{U} and \mathbf{C}_g are the vectors of the current speed and group velocity respectively, and $\omega =$ the wave frequency. For steady wave trains travelling in x -direction, the wave energy is calculated by $E = \rho g H^2 / 8$, this can be simplified as follow to obtain the wave height variation:

$$(\mathbf{U} + \mathbf{C}_g) \frac{H^2}{\omega} = \text{const.} \quad (11)$$

$$(\mathbf{U} + \mathbf{C}_g) \frac{H^2}{\omega + kU} = (\mathbf{C}_g) \frac{H_0^2}{\omega} \quad (12)$$

where $H =$ the wave height, $H_0 =$ the wave height at $\mathbf{U} = 0$, and $k =$ the wave number. For waves in rivers or propagation on ocean currents, by assuming that the current is uniform over the depth and the horizontal distance, and that it flows in the same direction as the waves, the wavelength variation is obtained from the usual irrotational dispersion relation as follows (Dean and Dalrymple, 1999):

$$(\mathbf{C} + \mathbf{U})^2 = \frac{g}{k} \tanh kd \quad (13)$$

where $\mathbf{C} =$ the phase speed, and $d =$ the water depth. Various currents were generated and superimposed with progressive waves produced by a wave generator in the studies of An and Shibayama (1994). The wave period was taken equal to $T = 1.01$ s, the wave height $H = 0.0298$ m, and the water depth $d = 0.3$ m, for all simulations. The domain was discretized by grids equal to $\Delta x = 0.012$ m in the x -direction, the depth of the domain was divided into 33 layers, and the time step was set to $\Delta t = 0.003$ s. Figure 3 shows the comparisons of the numerical prediction and analytical solution for the wave height and wave length variation for various current speeds on the fixed bed. It is seen that the influence of opposing currents has been shortening the wavelength and elongating the wave height. On the other hand, the influence of the following current shows a contrary tendency.

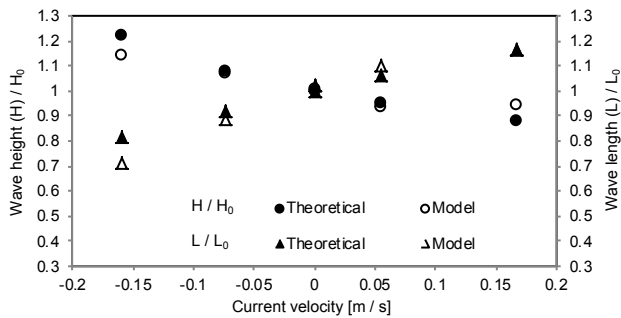


Figure 3. Wave height and wave length variations due to the current on the fixed bed.

4.3 Wave-Current Interaction on the Mud Bed

To validate the model, for the wave-current interaction on the muddy bed the experimental measurements conducted by An and Shibayama (1994) have been used. The experiments were carried out in a flume with a length of 17 m. The still water surface was at 0.263 m above the mud surface and the mud layer thickness was 0.08 m. The reported incident wave height of $H_0 = 0.045$ m and the wave period of $T = 1.01$ s have been applied for numerical simulations. A Bingham plastic rheology according to Papanastasiou's relationship was assumed for the bottom fluid mud layer with $\tau_y = 17$ N/m² and $\mu_B = 4.5$ Pa.s. The mud specific gravity was 2.08, and the water viscosity was taken equal to 1.0×10^{-6} m²/s. Numerical parameters were set as $\Delta x = 0.012$ m and $\Delta t = 0.003$ s, and the simulation time was set to 50 s. Water depth and the mud layer were divided into 24 and 8 layers respectively.

Figure 4 shows the comparison of the numerical simulations and laboratory measurements of two velocity profiles on the mud layer in two directions of current flow. The simulated and measured values of wave height and wave length variation are compared for various current speeds in Figures 5. Figure 6 shows the water wave heights variation along the channel on the mud layer. The effect of the currents on the wave attenuation coefficient (k_i) is illustrated in Figure 7, for numerical predictions and measured values, which shows good agreements. To estimate the wave attenuation quantitatively, an exponential decay law of wave height has been assumed.

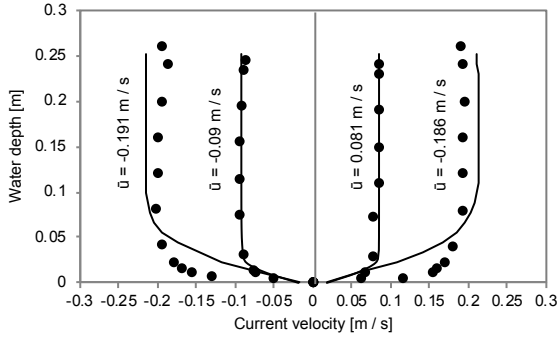


Figure 4. Velocity profiles of currents in opposing and following directions.

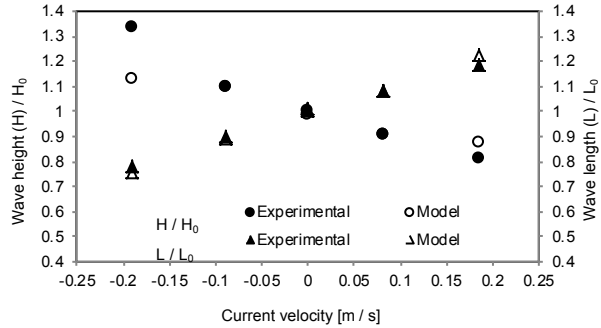


Figure 5. Wave height and wave length variation due to current on the mud bed.

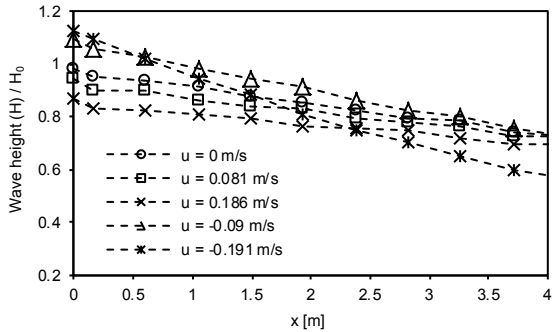


Figure 6. Water wave heights along the channel on the mud layer.

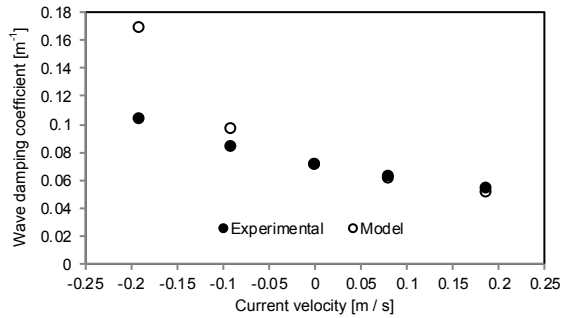


Figure 7. Effect of currents on wave attenuation coefficient on the mud layer.

5 DISCUSSION

For hydrodynamic tests, two free surface problems have been simulated. Horizontal component of flow velocity over a trench has been compared with the experimental data of Alfrink and van Rijn (1983). Although the curvatures of velocity profiles are not predicted exactly as the profiles of the measured values, model results in comparison with experimental data confirm the capability of the model in flow simulations with irregular bed geometry. According to the theoretical solution, the wave parameters change if the propagation of the regular wave on a fixed bed takes place with the following or opposing currents. This has been well predicted by the numerical simulations. The agreement with theoretical result is less for stronger opposite current, which may be due to the steepness of the wave produced, and the deficiency of the numerical model in exact simulation of this type of waves. Wave-current-mud interaction has been simulated for a two-layer system consisting of water and underlying fluid mud. The horizontal velocity profiles of currents in the water layer are rather similar to measurements of An and Shibayama (1994). The velocity values in the mud layer due to the current are negligible. Variations of the wave attenuation coefficient against current velocity and discrepancies with the experimental values for opposing current are related to the values of wave steepness.

6 CONCLUSIONS

A 2DV FVM numerical model has been utilized to investigate the interaction of wave, current and mud. The simulation of steady current over the trench in comparison with experimental measurements of velocity profiles shows good agreement. Wave height and wave length variations due to current on the fixed bed have been simulated satisfactory. On the mud bed, simulated results in accordance with measured values suggest that the wave length decreases in the opposing current and increases in the following current, while the wave height variations reveal an inverse tendency. This trend is also valid for the rate of wave attenuation in which k_i is greater in the opposing current and is less in the following current. It is seen that the opposing current has more significant effects on the rate of wave height attenuation than the following current.

NOTATION

C	the phase speed
C_g	the vector of group velocity
d	the water depth
E	the wave energy
g	gravity acceleration
H	the wave height
H_0	the wave height at $U=0$
k	the wave number
m	the material parameter
P^*	the pressure in the absence of hydrostatic pressure divided by reference density of water
t	time
U	the vector of current speed
u	the velocity
u_g	the vertical mesh velocity
x	the Cartesian coordinate
γ	the shear rate tensor
μ	the viscosity
μ_B	the plastic viscosity
ω	the wave frequency
ρ	fluid density
ρ_r	reference density of water
τ	the symmetric extra-stress tensor
τ_y	the yield stress

REFERENCES

- Alfrink, B.J., van Rijn, L.C. (1983). Two-equation turbulence model for flow in trenches. J. of Hydraulic Eng., ASCE, Vol. 109, No. 7, pp. 941-958.
- An, N.N. (1993). Mud mass transport under wave and current. Ph.D. dissertation, Dept. of Civil Eng., Yokohama National University, 135 pages.
- An, N.N., Shibayama, T. (1994). Wave-current interaction with mud bed. Coastal Engineering '94 - Proceedings of the 1994 Conference, G.V. Cotroneo and R.R. Rumer Editors, pp. 2913-2927.
- Bretherton, F.P., Garrett, C.J.R. (1969). Wavetrains in inhomogeneous moving media. Proceeding Royal Society of London, Sere A, Vol. 302, pp. 529-554.
- Dean, R.G., Dalrymple, R.A. (1991). Water wave mechanics for engineers and scientists. Academic Series on Ocean Engineering, vol 2. World Scientific, Singapore.
- Hejazi, K. (2005). 3D numerical modeling of flow and turbulence in oceanic water bodies using an ALE projection method. 1st Conference on Numerical Modeling in Civil Engineering, K.N. Toosi University of Tech., Tehran, pp. 47-99.
- Hejazi, K., Soltanpour, M., Sami, S. (2013). Numerical modeling of wave-mud interaction using projection method. Ocean Dynamics, Vol. 63, pp. 1093-1111.
- Papanastasiou, T.C. (1987). Flow of materials with yield. J. Rheology, Vol. 31, pp. 385-404.
- Thomas, G.P. (1981). Wave-current interactions: an experimental and numerical study. Part 1. Linear waves. Journal of Fluid Mechanics, Vol. 110, pp. 457-474.
- Tsuruya, H., Nakano, S., Takahama, J. (1987). Interaction between surface waves and a multi-layered mud bed. Rep. Port and Harbour Res. Inst., Ministry of Transport, Japan, Vol. 26, No.5, pp. 141-173.
- Zhao, Z.D., Lian, J.J., Shi, J.Z. (2006). Interactions among waves, current, and mud: Numerical and laboratory studies. Advances in Water Resources, Vol. 29, pp. 1731-1744.